# Eph:ephrin-B1 forward signaling controls fasciculation of sensory and motor axons

Maëva Luxey [a,b], Thomas Jungas [a,b], Julien Laussu [a,b], Christophe Audouard [a,b], Alain Garces [c], Alice Davy [a,b,*]

[a] Centre de Biologie du Développement, CNRS, 118 Route de Narbonne, 31062 Toulouse, France
[b] UPS, Université de Toulouse, France
[c] Institut des Neurosciences de Montpellier INSERM U-1051, Montpellier, France

## ARTICLE INFO

## ABSTRACT

Axon fasciculation is one of the processes controlling topographic innervation during embryonic development. While axon guidance steers extending axons in the accurate direction, axon fasciculation allows sets of co-extending axons to grow in tight bundles. The Eph:ephrin family has been involved both in axon guidance and fasciculation, yet it remains unclear how these two distinct types of responses are elicited. Herein we have characterized the role of ephrin-B1, a member of the ephrinB family in sensory and motor innervation of the limb. We show that ephrin-B1 is expressed in sensory axons and in the limb bud mesenchyme while EphB2 is expressed in motor and sensory axons. Loss of ephrin-B1 had no impact on the accurate dorso-ventral innervation of the limb by motor axons, yet *EfnB1* mutants exhibited decreased fasciculation of peripheral motor and sensory nerves. Using tissue-specific excision of *EfnB1* and in vitro experiments, we demonstrate that ephrin-B1 controls fasciculation of axons via a surround repulsion mechanism involving growth cone collapse of EphB2-expressing axons. Altogether, our results highlight the complex role of Eph:ephrin signaling in the development of the sensory-motor circuit innervating the limb.

## Introduction

A common feature of most axons in the nervous system is that they tend to grow along pre-existing neuronal projections thus forming thick bundles or nerves, which connect neuronal cell bodies and distant synaptic targets. Axon bundling, also called fasciculation, is an active process that requires both inter-axonal adhesion as well as contact repulsion provided by cues present in the environment. These adhesive and repulsive forces are modulated along nerve trajectories thus allowing axons to branch off the main fascicle at stereotypical positions called choice points. Attractive and repulsive axon guidance cues expressed in defined spatio-temporal patterns in the target tissue provide directional information to navigating axons and contribute to the establishment of neuronal circuits.

Unlike adhesion proteins which may act along the entire length of the axon, attractive and repulsive cues preferentially target a specialized domain of the axon called the growth cone. The growth cone is a highly motile and dynamic structure at the tip of the axon that constantly probes the environment via cell surface receptors that directly regulate local assembly or disassembly of the cytoskeleton (Lowery and Van Vactor, 2009). Attractive signals lead to stabilization of the cytoskeleton while repulsive cues destabilize the cytoskeleton and cause growth cone collapse.

Most contact repellant cues involved in axon fasciculation are also implicated in axon guidance, suggesting that both processes are dependent on each other and are regulated by similar molecular mechanisms (Kolodkin and Tessier-Lavigne, 2011). Yet, a number of studies suggest that these processes may be independent. For instance, it has been shown that specific Neuropilin/Semaphorin receptor/ligand pairs play distinct roles on both processes. While Sema3A-Npn-1 signaling controls both guidance and fasciculation of motor axon projections in the limb, Sema3F-Npn-2 functions as a guidance pair for a subset of motor axons but plays no role in their fasciculation (Huber et al., 2005). Conversely, Sema3F-Npn-2 signaling is required to drive fasciculation of the vomeronasal nerve but despite severe defasciculation most of the vomeronasal axons accurately innervate their target in *Sema3F* mutants (Cloutier et al., 2004). Even more strickingly, Slit2 has recently been implicated in fasciculation of motor axons innervating the diaphragm via an autocrine/juxtaparacrine mechanism that is distinct from its well known role as an environmental repulsive cue (Jaworski and Tessier-Lavigne, 2012).

* Corresponding author at: Centre de Biologie du Développement, CNRS, 118 Route de Narbonne, 31062 Toulouse, France.
  E-mail address: alice.davy@univ-tlse3.fr (A. Davy).

Eph receptors and ephrins belong to a family of cell surface proteins that exerts a well known but complex role in axon guidance: Eph and ephrins regulate axon guidance in two opposite ways, either as repulsive or as attractive cues, depending on the type of neurons (Egea and Klein, 2007; Feldheim and O'Leary, 2010). Complexity in this system arises from the fact that both Eph receptors and ephrins are competent to induce a transduction cascade upon interaction (respectively called "forward" and "reverse" signaling) thus acting both cell autonomously and cell non-autonomously (Davy and Soriano, 2005). Further, there are two classes of Eph receptors and ephrins (A and B) each regrouping several members which exhibit promiscuous binding preferences and partially redundant functions. Although Eph:ephrin signaling has been implicated in axon guidance and fasciculation, especially in the limb (Kao et al., 2011), the mechanisms involved are incompletely understood.

The sensory-motor circuit innervating the limb is composed of two types of neurons located in two distinct structures: motor neurons (MNs) which are located in the ventral horn of the spinal cord and receive inputs from the motor cortex; and sensory neurons (SNs) located in dorsal root ganglia (DRGs) which relay inputs from skin and muscles in the periphery towards spinal neurons including MNs (Bonanomi and Pfaff, 2010; Marmigere and Ernfors, 2007). During development, sensory and motor axons form tight bundles, a process which appears to be essential for accurate path finding in the limb. While a number of studies suggested that SNs depended on MN tracts for fasciculation and guidance, it has also been shown that SNs are able to fasciculate and innervate their proper targets in absence of MNs (Huettl et al., 2011; Wang and Scott, 1999). Conversely, MNs fasciculation in the limb was shown to be dependent on molecular cues present on SNs (Huettl et al., 2011). A number of genetic studies have shown that EphAs and ephrinAs are required for guidance and/or fasciculation of lateral motor column (LMC) axons innervating the limb (Helmbacher et al., 2000; Iwasato et al., 2007; Kania and Jessel, 2003; Kramer et al., 2006; Marquardt et al., 2005 ). In addition, EphA:ephrinA inter-axonal signaling is necessary to sort SNs and MNs projections within axial peripheral nerves (Gallarda et al., 2008) and to properly assemble these nerves (Wang et al., 2011). Although the role of class-B Eph/ephrins is less well characterized, pioneer studies had shown that ephrinBs expressed in the caudal half of somites serve as repulsive cues for EphB-expressing motor axons as they exit the spinal cord (Krull et al., 1997; Wang and Anderson, 1997) and recently, ephrin-B2, which is expressed both in the limb bud mesenchyme and in MNs, has been shown to control LMC axon guidance in the limb (Kao and Kania, 2011; Luria et al., 2008).

Herein we have characterized the role of another member of the ephrinB family, ephrin-B1, in sensory and motor innervation of the limb. We show that ephrin-B1 is expressed in sensory neurons as well as in the limb bud mesenchyme at the time motor and sensory axons invade this territory. Loss of ephrin-B1 had no effect on guidance of motor axons in the limb but peripheral nerves were defasciculated in *EfnB1* deficient embryos. Using a conditional loss-of-function genetic approach and in vitro experiments we demonstrate that ephrin-B1 promotes fasciculation by a surround repulsion mechanism involving growth cone collapse of EphB2-expressing axons.

## Material and methods

### Animals

Wild-type (*EfnB1^{wt}*) and *EfnB1* knock-out (*EfnB1^{ko}*) mice where generated as described (Davy et al., 2004) and kept in a mixed 129S4/C57BL/6J genetic background. The *Prx1-Cre* mouse line (Logan et al., 2002) was kept in a C57BL/6J pure background and mice carrying a floxed *EfnB1* allele (*EfnB1^{lox:lox}*) were described previously (Davy et al., 2004) and kept in a pure 129S4 genetic background. The *Hb9:GFP* mouse line was kept in a C57BL/6J pure background (Wichterle et al., 2002). All animal procedures were approved by the Midi-Pyrénées Animal Experimentation Ethics Committee (MP/07/21/04/11).

### HRP retrograde labeling of motor neurons

Retrograde labeling of motor neurons was performed as described (Luria et al., 2008). Briefly, the brachial region of E12.5 embryos was dissected and incubated in DMEM/F12 medium (GIBCO). The HRP solution was injected into either dorsal or ventral forelimb proximal muscle group and embryos were incubated at 37 °C and aerated with 5% $CO_2$. Fresh media was added every hour for 5 h. Embryos were fixed and process for immunostaining. Only embryos with clear inaccurate injection were discarded, which could result in a higher fraction of neurons with inappropriate identity, independently of genotype.

### Immunohistochemical staining

Embryos were fixed overnight at 4 °C in 4% PFA. After three washes in PBS/ Triton 0.5%, 70 or 100 μm vibratome sections were collected, blocked in PBS 1% BSA 0.1%Triton and incubated with primary antibodies overnight at 4 °C. Antibodies were as follows: ephrin-B1 and EphB2 (R&D Systems), EphA4 (Santa Cruz Biotech), phospho-tyrosine (Cell Signaling technology), βIII-tubulin (Covance), Islet1 (39.4D5; Hybridoma Bank), Foxp1 (Abcam), HRP (Jackson Immunoresearch), Tubulin (Hybridoma Bank) and Neurofilament (2H3, Hybridoma Bank). Primary antibodies were visualized by secondary antibodies conjugated with Alexa (Molecular probes) and applied for 1 h at room temperature with Draq5 as nuclear counterstaining (Vector Labs). Images were acquired either on a Nikon Eclipse 80*i* or on a Leica SP5 confocal except. Defasciculation was quantified by counting all *Hb9-GFP* or cutaneous Neurofilament-positive branches on at least 7° 100 μm-thick vibratome sections of the limb bud, for each embryo. Images of whole mount embryo preparations were acquired on a Nikon AZ100 binocular microscope. Nerve length was measured using the Image J software. The number of embryos of each genotype analyzed is indicated in the figure legends.

### In situ hybridization

In situ hybridization was performed on transverse vibratome sections of embryos collected at E11.5 and E12.5. Briefly, embryos were fixed 24 h in 4% paraformaldehyde (PFA), sectioned on the vibratome and sections were dehydrated in ethanol. Following rehydration, sections were treated with proteinase K (10 μg/ml in PBS/0.1% Tween-20) for 7 min at room temperature and subsequently post-fixed in PFA/glutaraldehyde solution. Sections were incubated overnight at 65 °C in hybridization buffer (50% formamide, $5 \times SSC$ (pH 6), 0.1% SDS, 50 μg/ml heparin, 500 μg/ml yeast RNA) containing the labeled probe. Sections were washed twice with solution I ($5 \times SSC$, 50% formamide, 0.1% SDS) at 65 °C and 3 times in solution III ($2 \times SSC$, 50% formamide, 0.1% SDS) at 65 °C, rinsed in TBS/0.1% Tween-20 and incubated overnight in blocking buffer (TBS with 2% goat serum, 0.1% blocking reagent (Roche), 0.1% Tween-20) containing an AP-labeled anti-DIG antibody (1/2000) (Roche). NBT/BCIP was used as a substrate for the Alkaline Phosphatase. For double labeling, in situ hybridization was followed by post-fixation
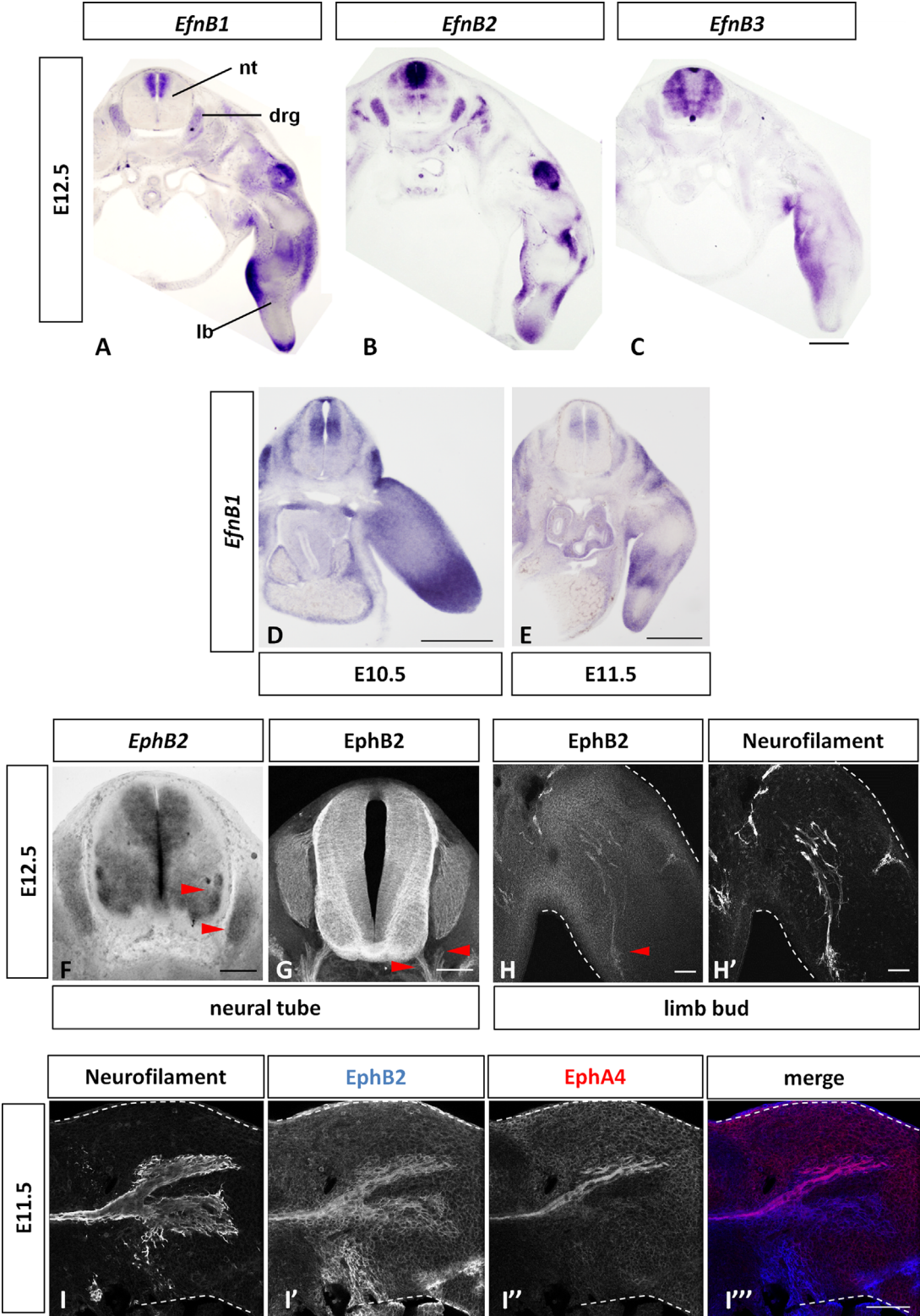
**Fig. 1.** Complementary expression of ephrin-B1 and EphB2 in the sensory-motor circuit innervating the limb. *A–C*, *EfnB1*, *EfnB2* and *EfnB3* mRNA expression in the neural tube and in the limb bud at E12.5. *D*, *E*, *EfnB1* mRNA expression detected by in situ hybridization on transverse vibratome sections of E10.5 and E12.0 embryos. *F* and *G*, Expression of EphB2 in the neural tube of E12.5 embryos detected by in situ hybridization (*F*) and immunofuorescence (*G*). EphB2 is expressed in motor and sensory projections (arrowheads). *H–H′*, Transverse vibratome sections of E12.5 embryos at forelimb level were stained for EphB2 (*H*) and Neurofilament (*H′*). Images are shown with dorsal to the top. *I–I″*, Transverse vibratome sections of the forelimb of E11.5 embryos were stained for Neurofilament (*I*), EphB2 (*I′*) and EphA4 (*I″*). *I‴*, Merged image of EphB2 and EphA4 stainings. The limb bud is shown with dorsal to the top. Scale bar (A–E) 1 mm; (F, G and I–I‴) 100 μm; (H–H′) 200 μm. nt: neural tube; drg: dorsal root ganglia; lb: limb bud.

(4% PFA for 30 min) and immunostaining was performed as described above.

### Explant and dissociated sensory neurons cultures

DRGs from E12.5 embryos were dissected in ice cold HBSS and plated on labteck II chambers (Nunc) coated with poly-ornithine containing 4 µg/ml of either IgG-Fc or ephrinB1-Fc recombinant proteins (R&D Systems). Explants were cultured for 16 h in Neurobasal medium (Invitrogen) with 0.5% Fetal Bovine serum, L-glutamine, Penicillin–streptomycin, Sodium Pyruvate and 50 ng/ml NGF7S (sigma). For dissociated sensory neurons, DRGs from E12.5 were collected in cold HBSS, resuspended in an enzymatic mix (1.3 mg/ml Trypsin, 0.7 mg/ml TypeI-S-hyaluronidase and 0.13 mg/ml Kynurenic acid in HBSS) (Sigma) for 2 min at 37 °C, rinsed in Neurobasal medium and plated on poly-ornithine coated labteck II chambers in Neurobasal medium (Invitrogen) with 0.5% Fetal Bovine serum, L-glutamine, Penicillin-streptomycin, Sodium Pyruvate and 50 ng/ml NGF7S (Sigma) (Kirkham et al., 2006). Sensory neurons were cultured for 16 h and exposed to fresh media containing 4 µg/ml of either IgG-Fc or ephrinB1-Fc recombinant proteins for 30 min at 37 °C. Explants or dissociated SNs were fixed in 2% PFA for 10 min and immunostained as described

above. Quantification of neuritic fasciculation was performed using the ImageJ software. Fasciculation was quantified by measuring the surface covered by neurites around each DRG explant (number of pixels corresponding to the DRG explants substracted from the total number of pixels corresponding to DRG explants+neurites). The graph represents an average number of pixels. The data was collected from three independent experiments. The number of DRG explants analyzed in each condition is indicated in the figure legends. Quantification of growth cone collapse was done manually on neurons from three independent primary neuronal cultures and double-stained for actin and β-tubulin. Growth cones with 2 or fewer filipodia were considered collapsed. The number of growth cones analyzed is indicated in the figure legends.

### Time lapse microscopy

Sensory neurons were plated on labteck II chambers (Nunc) coated with poly-ornithine containing 4 µg/ml of either IgG-Fc or ephrinB1-Fc recombinant proteins (R&D Systems). Cultures were maintained at 37 °C in a humidified chamber containing 5% $CO_2$
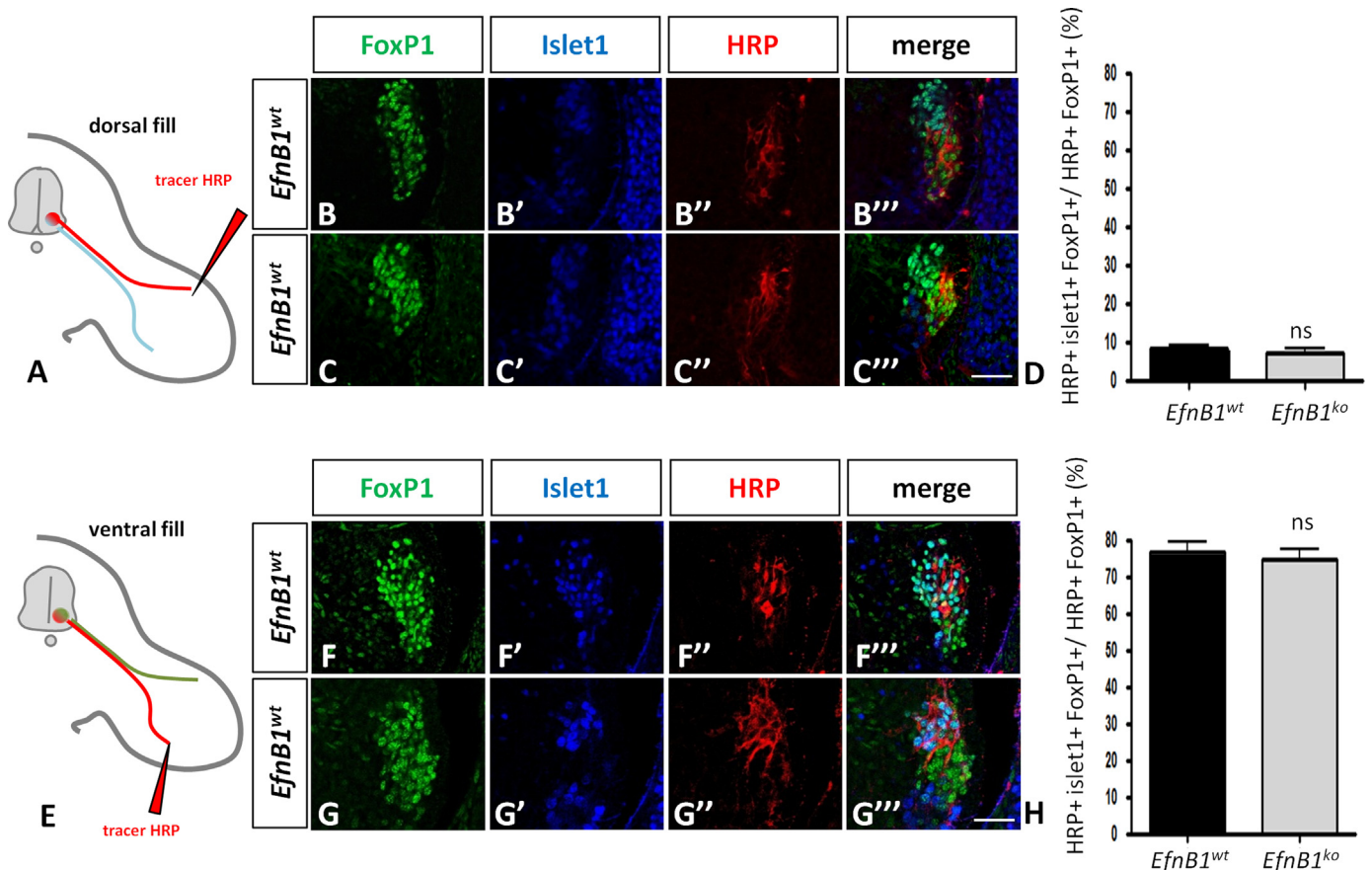


Fig. 2. Ephrin-B1 is not required for accurate dorso-ventral innervation of the limb. **A**, Schematic representation of dorsal retrograde labeling. **B–B′′′**, wild type motor projections targeting the dorsal half of the forelimb were backfilled with HRP and MNs soma were immunostained for Foxp1 (**B**), Islet1 (**B′**) and HRP (**B′′**). **C–C′′′**, $EfnB1^{ko}$ motor projections targeting the dorsal half of the forelimb were backfilled with HRP and MNs soma were immunostained for Foxp1 (**C**), Islet1/2 (**C′**) and HRP (**C′′**). **D**, Quantification of the ratio between HRP+/Islet1+/Foxp1+ projections and HRP+/Foxp1+ projections in $EfnB1^{wt}$ (8,250 ± 1,014; $n=48$ sections from 5 embryos) and $EfnB1^{ko}$ (7,007 ± 1,156; $n=18$ sections from 3 embryos) embryos. $p$-value > 0.05, non significant, two-tailed $t$-test. **E**, Schematic representation of ventral retrograde labeling. **F–F′′′**, wild type motor projections targeting the ventral half of the forelimb were backfilled with HRP and MNs soma were immunostained for Foxp1 (**F**), Islet1 (**F′**) and HRP (**F′′**). **G–G′′′**, $EfnB1^{ko}$ motor projections targeting the ventral half of the forelimb were backfilled with HRP and MNs soma were immunostained for Foxp1 (**G**), Islet1 (**G′**) and HRP (**G′′**). **H**, Quantification of the ratio between HRP+/Islet1+/Foxp1+ projections and HRP+/Foxp1+ projections in $EfnB1^{wt}$ (76,74 ± 2,563; $n=15$ sections from 3 embryos) and $EfnB1^{ko}$ (74,61 ± 2,692; $n=21$ sections from 4 embryos) embryos. $p$-value > 0.05, non significant, two-tailed $t$-test. Scale bars for all images 50 µm. ns: non significant.

and images were acquired on an inverted microscope (Zeiss). Images were recorded after 5 h of culture (t0) using a video camera (one image every 15 min) for approximately 16 h.



## Results

*The EphB2/ephrin-B1 pair is expressed in complementary patterns in the sensory-motor circuit in the limb.*

We examined the expression pattern of ephrin-B1 in the developing spinal cord and in the limb bud at various stages of development encompassing specification and axonal navigation of SNs and MNs (E10.5 and E12.5). First we compared the expression pattern of ephrin-B1 with that of the other two members of the ephrin-B family at E12.5, when motor and sensory projections have crossed the plexus region and invade the most distal part of the limb bud. Amongst the 3 ephrinBs, ephrin-B1 is the most strongly expressed in the mouse limb bud (Fig. 1A–C). At this stage the expression pattern of *EfnB1* in the limb bud is complex, with higher expression domains at the distal tip and in a ventral region of the limb bud, yet expression of *EfnB1* is detected throughout the limb bud mesenchyme. In addition, *EfnB1* is weakly expressed in the axial mesenchyme surrounding the spinal cord. At E12.5, *EfnB2* is expressed in discrete domains in the limb bud, partly over-lapping *EfnB1*-positive territories (Fig. 1B). Expression of *EfnB3* is detected in a ventral region of the limb bud (Fig. 1C). At E10.5, *EfnB1* is expressed throughout the limb mesenchyme in a proximo-distal gradient (Fig. 1D). At E11.5, expression of *EfnB1* becomes regionalized in the limb bud with slightly stronger ventral expression (Fig. 1E). In addition to their mesenchymal expression, *EfnB1* and *EfnB2* are expressed in DRGs which contain the cell bodies of SNs (Fig. 1A and B). No *EfnB1* expression was detected in the ventral horn of the spinal cord, suggesting that ephrin-B1 is not expressed in MNs (Fig. 1A, D and E). Immunos-taining confirmed that ephrin-B1 is expressed in SNs but not in MNs (Figure S1A–A‴). EphB2, one of the preferred cognate receptors for ephrin-B1, is expressed in MNs and in SNs, as shown by in situ hybridization (Fig. 1F) and immunostaining (Fig. 1G). EphB3 and EphA4 which can also interact with ephrin-B1 are also expressed in MNs and SNs (Fig. S1B and C). Unlike EphA4 which is restricted to dorsally projecting axons, EphB2 is expressed on all peripheral projections innervating the limb at all stages analyzed (Fig. 1H–I‴ and Fig. S1D-D‴). Co-labeling of ephrin-B1 and axonal projections revealed that growing nerves invade ephrin-B1-positive territories as they navigate in the limb (Fig. S1E). Alto-gether, these expression patterns suggest that ephrin-B1:EphB2 signaling could play a role in sensory-motor innervation of the limb.

*Ephrin-B1 is required for fasciculation but not dorso-ventral guidance of motor axons in the limb.*

To investigate this putative role of ephrin-B1:EphB2 signaling, we analyzed sensory and motor innervation of the limb in genetically modified mice deficient for *EfnB1* (*EfnB1^ko*) (Davy et al., 2004). First, we performed retrograde labeling of MNs

**Fig. 3.** Defasciculation of motor axons in *EfnB1^ko* mutant embryos. **A**, Schematic view of a transverse section of mouse embryo at brachial level. **B–C**, Transverse sections of the forelimb of E12.5 *EfnB1^wt* (**B**) and *EfnB1^ko* (**C**) embryos carrying the *Hb9:GFP* transgene (green) and stained with Draq5 (blue). Motor projections (green) are defasciculated in *EfnB1* mutant embryos (bracket) compared to controls. **D**, **E**, Transverse sections at brachial level of E12.5 *EfnB1^wt* (**D**) and *EfnB1^ko* (**E**) embryos carrying the *Hb9:GFP* transgene (green) and stained with Islet1 (blue). Axial motor projections (green) are defasciculated in *EfnB1* mutant embryos (asterisks, **E**) compared to controls (**D**). **F**, Quantification of the total number of motor nerves branches/per section in *EfnB1^wt* (black bar; n=6) and *EfnB1^ko* mutant embryos (gray bar; n=4). p-value=0.0095, ***, two tailed *T*-test. **G–H**, Transverse sections at thoracic level of E12.5 wild type and *EfnB1^ko* embryos carrying the *HB9:GFP* transgene (green) and stained with Draq5 (blue). Motor axons misproject in DRGs in *EfnB1^ko* embryos (arrowhead, **H**) (n=4/4). Scale bars for all images 100 μm.
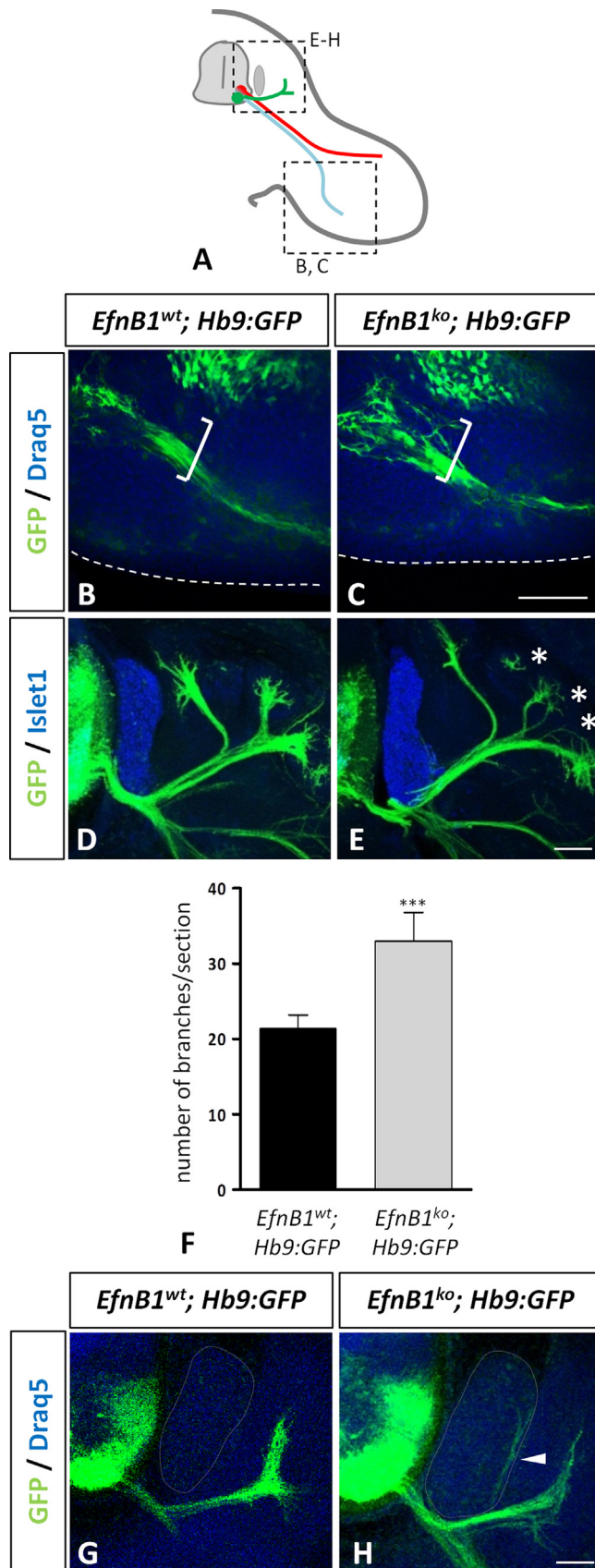
projecting to the limb to evaluate whether ephrin-B1 is required for accurate dorso-ventral innervations, as was shown for ephrin-B2 (Luria et al., 2008). Motor neurons of the LMC express Foxp1 and MNs innervating the ventral half of the limb express Islet1 whereas LMC MNs innervating the dorsal half of the limb are Islet1-negative and express the transcription factor Lim1 (Tsuchida et al., 1994). Neither ventral nor dorsal backfill revealed significant changes in the proportion of HRP-labeled Islet1-positive vs. Islet1-negative MNs in *EfnB1*$^{ko}$ compared to wild type controls (Fig. 2), indicating that ephrin-B1 is not required for the guidance of LMC motor axons at this primary dorso-ventral choice point.

We next investigated whether loss of ephrin-B1 may affect fasciculation of motor axons using the *Hb9:GFP* reporter allele to trace motor nerves. We first focused on projections innervating the ventral aspect of the limb where ephrin-B1 is highly expressed. In *EfnB1*$^{ko}$, motor projections were defasciculated compared to control embryos (Fig. 3B and C). Defasciculation was not limited to the limb as motor projections at axial level exhibited surnumerary branches (Fig. 3D and E). This phenotype was quantified by counting the total number of *Hb9:GFP*-positive branches per section (Fig. 3F). In addition, ectopic branches improperly invading DRGs could be observed in *EfnB1*$^{ko}$ embryos (Fig. 3G and H). Altogether these results
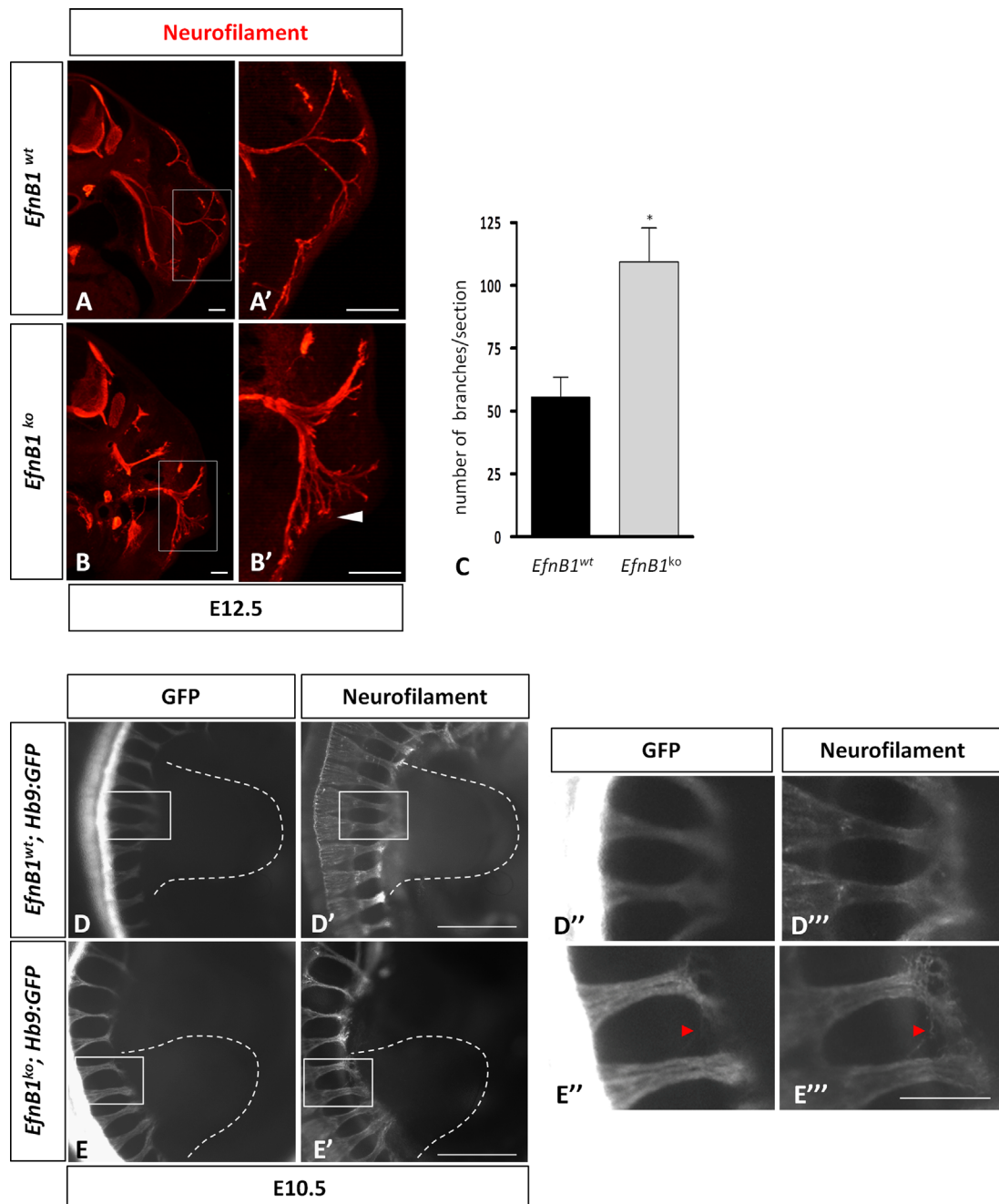


Fig. 4. Defasciculation of sensory axons in *EfnB1*$^{ko}$ mutant embryos. **A–B**′, Transverse sections of the forelimb of E12.5 *EfnB1*$^{wt}$ (**A**, **A**′) and *EfnB1*$^{ko}$ (**B**, **B**′) embryos were stained for Neurofilament. **A**′, **B**′, High magnification of the areas boxed in (**A**, **B**) show defasciculation of sensory neurons in the dermis in *EfnB1* mutant embryos (arrowheads). **C**, Quantification of the number of neurofilament-positive branches per section in *EfnB1*$^{wt}$ (black bar) and *EfnB1*$^{ko}$ embryos (gray bar) (n=4 embryos of each genotype). p-value=0.0137, *, two tailed t-test. **D–E**′′′, E10.5 *EfnB1*$^{wt}$ (**D–D**′′) and *EfnB1*$^{ko}$ (**E-E**′′′) whole embryos carrying the *HB9:GFP* transgene (GFP, **D**, **E**, **D**″ and **E**″) were stained for Neurofilament (**D**′, **E**′, **D**′′′ and **E**′′′). **D**″–**E**′′′, High magnification images of the boxed areas in (**D**, **D**′, **E** and **E**′). Defasciculated motor (red arrowhead) are detected in *EfnB1* mutant embryos (n=4/4). Scale bars (A and B′) 100 μm; (D–E′) 1 mm; (D′′–E′′′) 450 μm.

suggest that ephrin-B1:EphB2 signaling is required for proper fasciculation of motor axons.

*EfnB1^{ko} mutant embryos exhibit defects in sensory axon fasciculation.*

To test whether the loss of ephrin-B1 specifically impacted motor projections, we analyzed sensory projections targeting the dermis. At E12.5, peripheral projections in the dermis exhibited exuberant branching in *EfnB1^{ko}* (Fig. 4A–B′), a phenotype which was quantified by counting the total number of branches (Fig. 4C and Fig. S2A–B′). To test whether this phenotype was due to precocious or exuberant axonal extension, we examined peripheral projections at earlier developmental stages. At E10.5, growth of spinal nerves towards the plexus seemed slightly delayed in *EfnB1^{ko}* (Fig. 4D–E′) which correlated with a shorter length of spinal nerves (Fig. S2C–E). More importantly, defasciculated spinal nerves innervating the upper limb could be observed in mutant embryos (13/30 in *EfnB1^{ko}* compared to 2/32 in *EfnB1^{wt}*, $n=4$ embryos per genotype). Motor and sensory defasciculated branches could be observed in proximal and distal regions of the nerves (Fig. 4E″–E‴ and Fig. S2C and D). Altogether these results indicate that absence of ephrin-B1 led to defasciculation of both sensory and motor peripheral nerves.

*Ephrin-B1 controls axon fasciculation in a non-cell autonomous manner.*

Since fasciculation of sensory and motor axons are partly dependent on each other (Huettl et al., 2011) and ephrin-B1 is expressed in SNs, a possible explanation for the observed defasciculation of both SNs and MNs in *EfnB1^{ko}* could be that ephrin-B1:Eph inter-axonal signaling promotes adhesion of sensory fibers. Alternatively, ephrin-B1 expressed in the environment (SNs or mesenchymal cells) could promote axon fasciculation of SNs and MNs via a surround repulsion mechanism. To discriminate between these possible modes of action, we excised *EfnB1* specifically in mesenchymal cells in the limb bud using *Prx1-Cre* mice (Logan et al., 2002) and *EfnB1^{flox/flox}* mice (Davy et al., 2004). As expected, we observed that *EfnB1* was no longer expressed in the forelimb mesenchyme of E12.5 *EfnB1^{Y/lox}; Prx1-Cre* embryos (Fig. 5A and B). Interestingly, similar to *EfnB1^{ko}* embryos, conditional mutant embryos exhibited an increased number of Neurofilament-positive branches in the limb bud (Fig. 5C) and defasciculation of peripheral projections targeting the ventral aspect of the limb could be detected (Fig. 5D–E″). Altogether, these results show that expression of ephrin-B1 is required in mesenchymal cells to direct fasciculation of peripheral projections in the limb possibly by a surround repulsion mechanism.
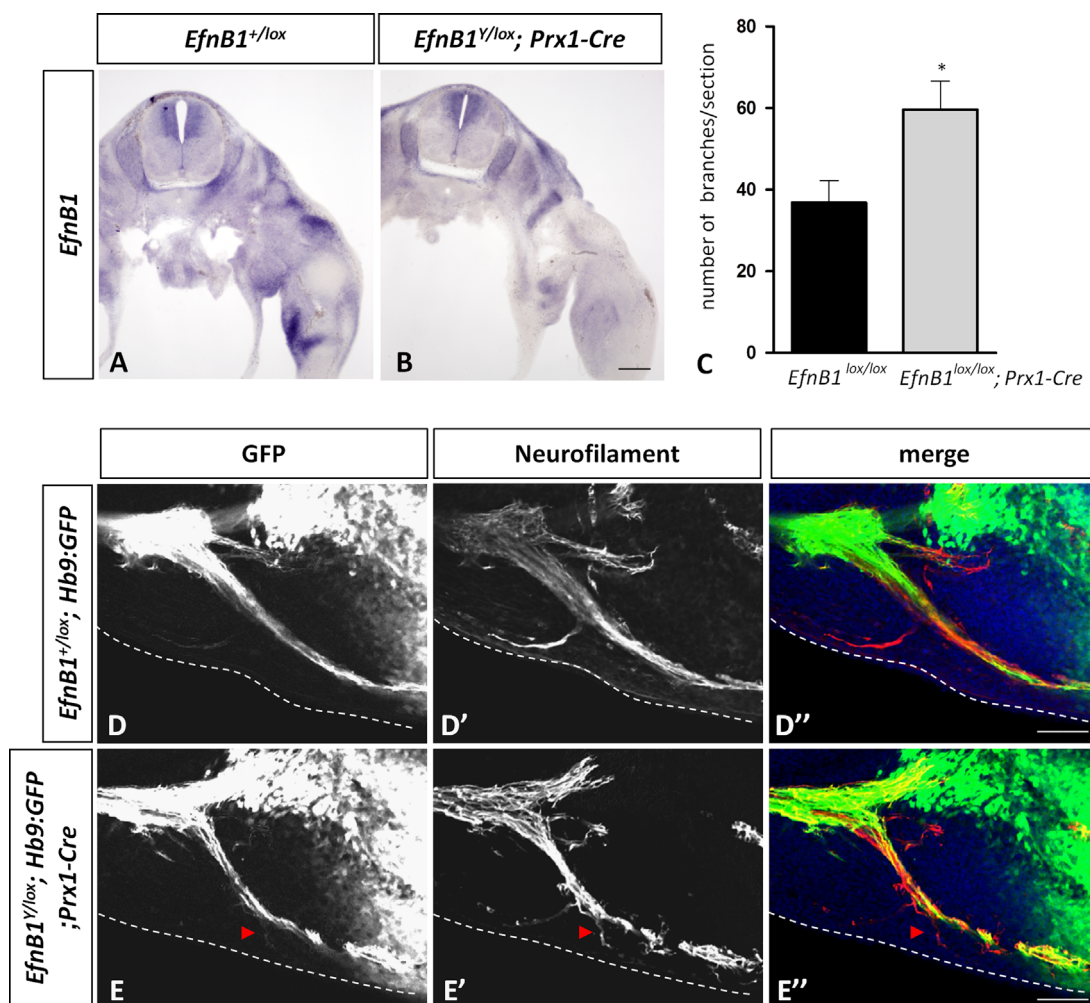


**Fig. 5.** Mesenchymal ephrin-B1 promotes axon fasciculation. **A–B**, *EfnB1* mRNA expression detected by in situ hybridization on transverse sections of *EfnB1^{lox/lox}* and *EfnB1^{lox/lox}; Prx1-Cre* E12.5 mouse embryos at brachial level. **C**, Quantification of the number of Neurofilament-positive branches per section in control (black bar; $n=4$) and *EfnB1^{lox/lox}; Prx1-Cre* mutant embryos (gray bar; $n=5$). p-value=0.0491, *, two tailed t-test **D–E″**, Transverse sections at the forelimb level of E12.5 *EfnB1^{+/lox}* (**D–D″**) or *EfnB1^{lox/lox}; Prx1-Cre* (**E–E″**) mouse embryos carrying the *HB9:GFP* transgene (GFP, **D** and **E**) were stained for Neurofilament (**D′** and **E′**). Draq5 was used to label nuclei in (**D″–E″**). Defasciculated motor branch (arrowhead) are detected in *EfnB1* mutant embryos ($n=3/4$). The limb bud is shown with dorsal to the top. Scale bar (A and B) 1 mm; (D–E″) 100 μm.

## Environmental ephrin-B1 promotes growth cone collapse

To confirm that ephrin-B1 functioned as an environmental cue to direct fasciculation of peripheral projections, we isolated DRG explants from E12.5 wild type embryos and evaluated their ability to extend neurites in presence or absence of ephrin-B1 in the environment. First, we analyzed expression of ephrin-B1 and EphB2 in these explants. While EphB2 expression could be readily detected in DRG explants (Fig. 6A–A″), expression of ephrin-B1 was lost (Fig. S3A–A″). Next, we established that stimulation with ephrin-B1 would activate forward signaling in sensory neurites (Fig. S3B–C‴). Using markers for the actin and microtubule cytoskeletons to label growing neurites, we observed that the majority of sensory neurites extending on a substrate containing ephrinB1-Fc were highly fasciculated (Fig. 6C–C″, E–E″ and F) whereas the majority of sensory neurites growing on control conditions remained defasciculated (Fig. 6B–B″, D–D″ and F). These results suggest that Eph-expressing neurites tend to fasciculate with each other in order to limit their contact with the ephrin-B1-coated substrate and imply that ephrin-B1 acts as a repulsive cue for EphB2-expressing neurites.

We next tested the putative role of ephrin-B1 as a repulsive cue for sensory axons using two paradigms: first, isolated SNs were cultured on surface-coated ephrinB1-Fc for 16 h and various parameters of neurite growth were recorded by live imaging. Second, isolated SNs were exposed acutely to soluble ephrinB1-Fc and the consequence of this treatment on growth cone morphology was assessed by immunofluorescence on fixed samples. Plating of isolated SNs on a substrate containing ephrinB1-Fc led to a significant increase in the proportion of neurons that did not extend a neurite compared to SNs plated on control substrate (Fig. 7A). However, for neurons that do extend a neurite, the speed of neuritic growth was unaffected by coating conditions (Fig. 7B and C). These results suggest that ephrin-B1 exerts a neurite growth inhibitory function for a subset of SNs. Consistent with this, acute activation of forward signaling in dissociated SNs led to a significant increase in the fraction of collapsed growth cones (Fig. 7D–F). Altogether these results demonstrate that ephrin-B1 acts as a repulsive cue for sensory axons.

## Discussion

### EphB:ephrinB signaling in axon fasciculation

Here we showed that loss of ephrin-B1 leads to defasciculation of both sensory and motor peripheral projections. Tissue-specific excision of *EfnB1* in mesenchymal cells of the limb was sufficient to induce defasciculation of peripheral projections, indicating that ephrin-B1 controls fasciculation via a surround repulsion mechanism. Defasciculation of sensory axons has been shown to induce defasciculation of motor axons in a *Npn-1* mutant background (Huettl et al., 2011), it is thus possible that sensory projections are the primary targets of ephrin-B1:EphB2-induced fasciculation and that motor projections are affected indirectly. Further, because defasciculation of both sensory and motor projections was more robust in full knock-out embryos compared to conditional knock-out embryos, we cannot completely rule out that expression of ephrin-B1 in sensory axons also promotes their fasciculation via a mechanism distinct from surround repulsion.

Our results indicate that ephrin-B1 controls axon fasciculation, at least in part, by activating EphB2 forward signaling in growing axons and promoting growth cone collapse. A role for EphB1, EphB2 and EphB3 in the choice of dorso-ventral motor innervation of the limb has been reported previously (Luria et al., 2008), however fasciculation of motor and/or sensory projections was not analyzed in this study. On the other hand, it has been shown that *EphB2⁻/⁻/EphB3⁻/⁻* mutant mice
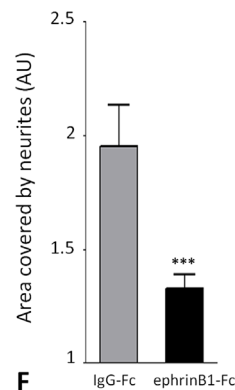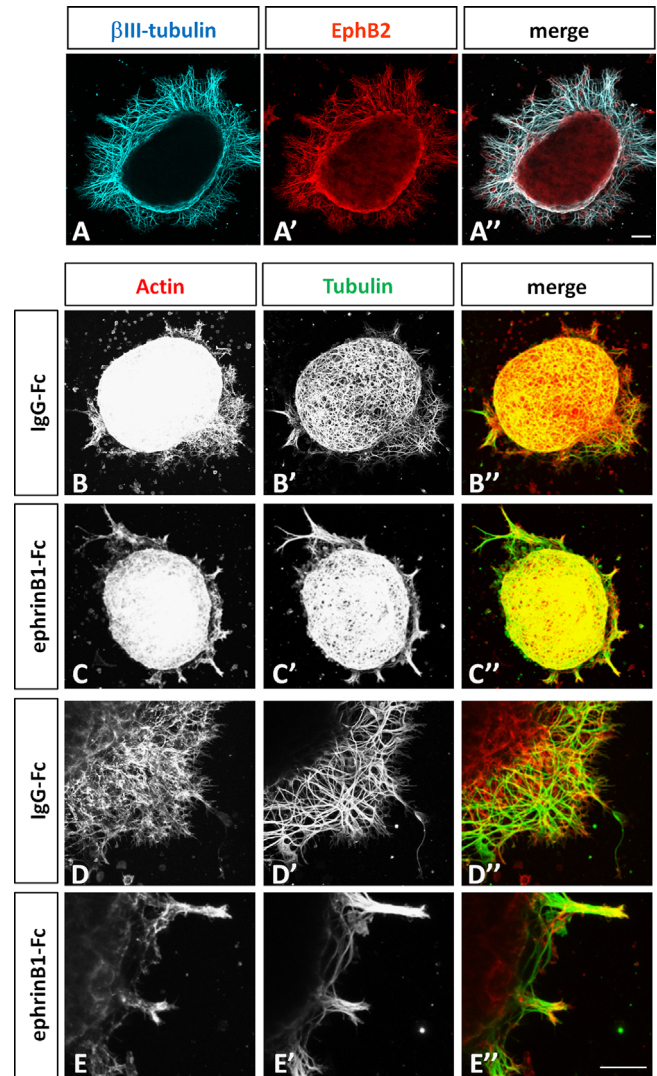


**Fig. 6.** Ephrin-B1 forward signaling promotes neuritic fasciculation in cultured DRG. **A–A″**, DRG explants were immunostained for β3-tubulin (**A**) and EphB2 (**A′**). **B–E″**, DRG explants from E12.5 wild type embryos were grown on IgG-Fc (**B–B″** and **D–D″**) or ephrinB1-Fc (**C–C″** and **E–E″**) coated Labteck chambers and stained for actin (**B**, **C**, **D** and **E**; red) and Tubulin (**B′**, **C′**, **D′**, **E′**; green). **D-E″**, High magnification images show the fasciculation of neurites growing on ephrinB1-Fc compared to neurites growing on IgG-Fc. **F**, Quantification of neuritic fasciculation in DRGs cultured on IgG-Fc (*n*=15) or on ephrinB1-Fc (*n*=22). *p*-value < 0.001, ✱✱✱, unpaired *t*-test. Scale bar (A–A″) 20 μm; (B–C″) 100 μm; (D–E″) 50 μm.

exhibit defasciculation of the habenular-interpeduncle tract (Orioli et al., 1996) and of the optic nerve (Birgbauer et al., 2000), which supports our conclusions that EphB2 forward signaling is required for
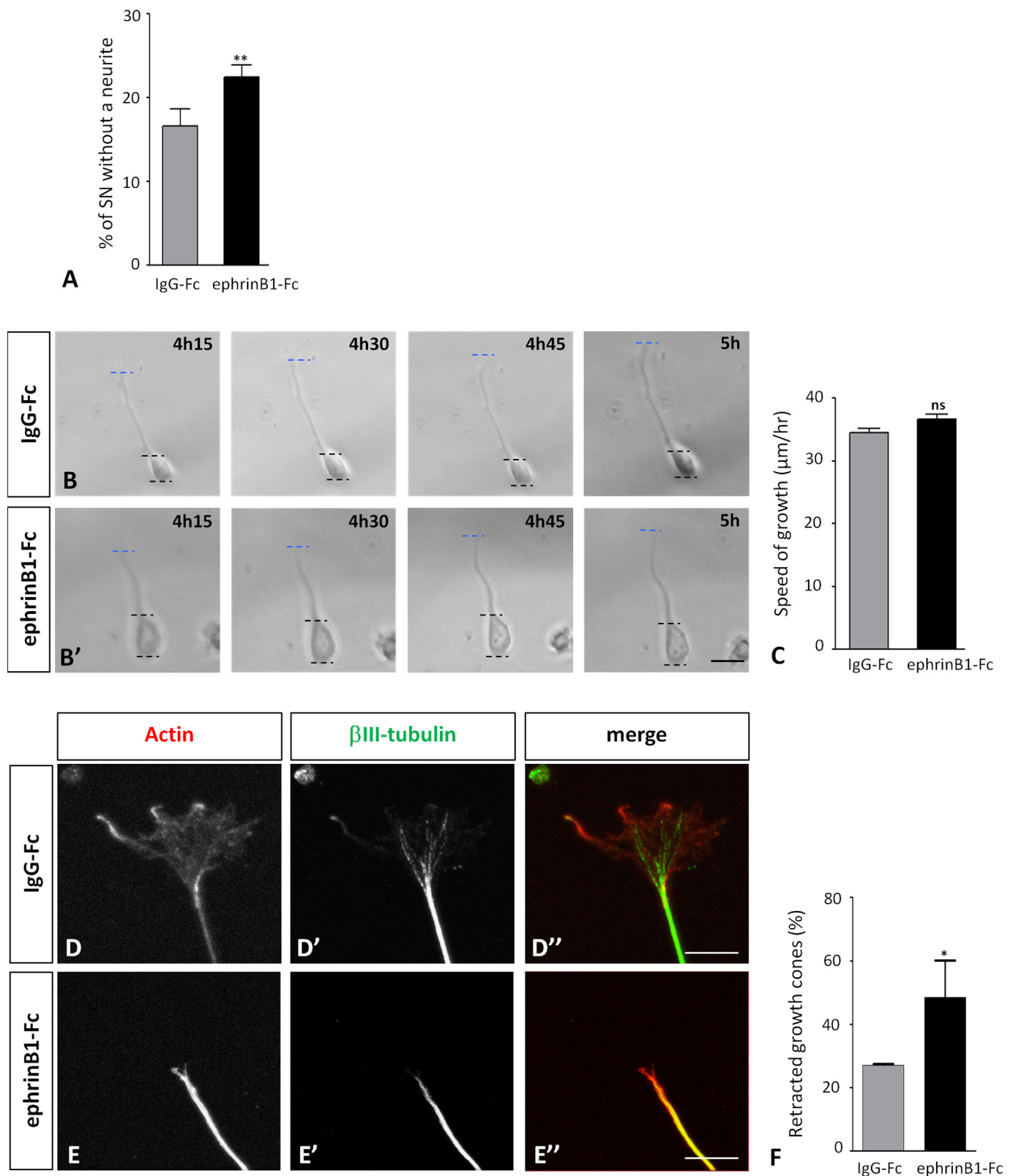
**Fig. 7.** Ephrin-B1 promotes collapse of sensory growth cones. ***A***, Percentage of sensory neurons cultured on IgG-Fc or on ephrinB1-Fc that do not extend a neurite. At least 450 sensory neurons distributed on 6 cultures were counted. ***B*** and ***B′***, Still images taken from a movie of sensory neurons cultured either on IgG-Fc (***B***) or on ephrinB1-Fc (***B′***). Black bars delineate soma while blue bars mark the extremity of neurites. Scale bar 10 μm. ***C***, Quantification of speed of neuritic growth on neurons cultured on IgG-Fc ($n=190$) or ephrinB1-Fc ($n=200$). Statistical analysis was performed using Mann and Whitney unpaired test (**=$p$-value $< 0.01$). ns: non significant. ***D–E″***, Isolated sensory neurons stimulated either with IgG-Fc (***D–D″***) or with ephrinB1-Fc (***E–E″***) were double stained for F-actin (***D*** and ***E***; red) and β3-tubulin (***D′*** and ***E′***; green). ***F***, Percentage of retracted growth cone upon bath application of IgG-Fc or ephrinB1-Fc. Statistical analysis was performed comparing IgG-Fc stimulated values vs. ephrinB1-Fc stimulated values collected on three independent experiments. At least 50 growth cones were counted per condition for each experiment. $p$-value $< 0.05$, *, unpaired $t$-test. Scale bar (A–A″) 20 μm, (D–E″) 10 μm. ns: non significant.

axon fasciculation. Another candidate receptor to mediate ephrin-B1 surround repulsion could have been EphA4 as defasciculation of motor branches innervating the hindlimbs have been observed in some $EphA4^{-/-}$ mutants (Helmbacher et al., 2000) and EphA4 is a cognate receptor for ephrin-B1 (Arvanitis et al., 2013; Noberini et al., 2012; North et al., 2009). However, we show here that loss of ephrin-B1 induces defasciculation of nerves projecting ventrally in the limb and that these nerves express low levels of EphA4, supporting the idea that EphB2 is the preferred receptor to mediate ephrin-B1-induced fasciculation. Interestingly, we observed an ectopic invasion of DRGs by motor projections in $EfnB1^{ko}$, which is reminiscent of the misrouting phenotype observed in $EphA3^{-/-}/EphA4^{-/-}$ mutants (Gallarda et al., 2008). This phenotype was attributed to a loss of transaxonal repulsive signaling between ephrin-A5 expressed on sensory axons and EphA3/EphA4 expressed on motor axons. Similarly, the ectopic projection of motor axons in DRGs that we observed in $EfnB1^{ko}$ could be due to a loss of repulsive signaling between ephrin-B1 expressed on sensory axons and EphB2 expressed on motor projections.

*Axon fasciculation vs. axon guidance*

Another member of the ephrinB family, ephrin-B2 is expressed in the limb bud mesenchyme and has been involved in specifying dorso-ventral motor axon trajectories in the limb in cooperation with EphB1-B3 receptors (Kao and Kania, 2011; Luria et al., 2008). Here we show that unlike ephrin-B2, ephrin-B1 seems to have a general role in axon fasciculation rather than in guidance at choice points. This general role of ephrin-B1 in axon fasciculation is highlighted by the fact that defasciculation also affects cranial nerves in $EfnB1^{ko}$ (Davy et al., 2004). These results indicate that ephrin-B1 and ephrin-B2 cannot compensate for each other despite partially overlapping expression patterns in the limb and in DRGs and suggest that different ephrins may perform complementary rather than redundant functions during innervation of the limb. One possible explanation for the differential outcomes of ephrin-B1 vs. ephrin-B2 forward signaling could be linked to the different binding affinities of both ligands for EphB2. Indeed ephrin-B2 binds EphB2 with higher affinity than ephrin-B1 (Noberini et al., 2012), which could lead to different signaling strength and thus to different biological outcomes. A differential effect of ephrin-B1 and ephrin-B2 on growth cone collapse has been reported recently for cortical neurons (Srivastava et al., 2013). In addition, it has been shown that ephrin-B2 forward signaling elicits different collapse responses in ventral vs. dorsal retinal ganglion cells that express different levels of EphB2 (Petros et al., 2010 ). Similar to these results on ephrin-B1 and ephrin-B2, distinct roles on axon guidance and fasciculation of spinal motor axons have been reported for two members of the Semaphorin family. While Sema3A-Npn1 signaling mediates fasciculation and guidance of LMC motor axons, Sema3F-Npn2 only plays a role in guidance of medial LMC axons but is not required for their fasciculation (Haupt et al., 2010; Huber et al., 2005). In addition, it has been shown in vitro using MNs derived from embryonic stem cells that different doses of Sema3A and Sema3F elicit different responses in growth cones (Nédelec et al., 2012 ). It is thus tempting to speculate that gradation in the response to repulsive cues, either based on exposure doses or on receptor-ligand affinity, could be a switch mechanism between guidance at choice points and fasciculation.

One intriguing question that arises from our studies concerns pioneer axons. Indeed, our data shows that EphB2-positive projections invade ephrin-B1-positive territories, suggesting that pioneer axons must be insensitive to ephrin-B1 induced growth cone collapse. One possible explanation for this could be that pioneer axons in the limb are motor axons (Landmesser and Honig, 1986; Tosney and Landmesser, 1985) which could be less sensitive to ephrin-B1-induced growth cone collapse and thus provide a scaffold to sensory axons.

Altogether, our study highlights the multistep control Eph:ephrin signaling exerts on the development of the sensory-motor circuit innervating the limb and suggests that different ephrins may have specific as well as redundant biological functions.

### Appendix A. Supporting information

Supplementary data associated with this article can be found in the online version at http://dx.doi.org/10.1016/j.ydbio.2013.09.010.

### References

Arvanitis, D.N., et al., 2013. Ephrin-B1 maintains apical adhesion of neural progenitors. Development 140, 2082–2092.

Birgbauer, E., et al., 2000. Kinase independent function of EphB receptors in retinal axon pathfinding to the optic disc from dorsal but not ventral retina. Development 127, 1231–1241.

Bonanomi, D., Pfaff, S.L., 2010. Motor axon pathfinding. Cold Spring Harb Perspect. Biol. 2, a001735.

Cloutier, J.F., et al., 2004. Differential requirements for semaphorin 3F and Slit-1 in axonal targeting, fasciculation, and segregation of olfactory sensory neuron projections. J. Neurosci. 24, 9087–9096.

Davy, A., et al., 2004. EphrinB1 forward and reverse signaling are required during mouse development. Genes Dev. 18, 572–583.

Davy, A., Soriano, P., 2005. Ephrin signaling in vivo: look both ways. Dev. Dyn. 232, 1–10.

Egea, J., Klein, R., 2007. Bidirectional Eph-ephrin signaling during axon guidance. Trends Cell Biol. 17, 230–238.

Feldheim, D.A., O'Leary, D.D., 2010. Visual map development: bidirectional signaling, bifunctional guidance molecules, and competition. Cold Spring Harb. Perspect. Biol., a001768. (Epub).

Gallarda, B.W., et al., 2008. Segregation of axial motor and sensory pathways via heterotypic trans-axonal signaling. Science 320, 233–236.

Haupt, C., et al., 2010. Semaphorin 3A-Neuropilin-1 signaling regulates peripheral axon fasciculation and pathfinding but not developmental cell death patterns. Eur. J. Neurosci. 31, 1164–1172.

Helmbacher, F., et al., 2000. Targeting of the EphA4 tyrosine kinase receptor affects dorsal/ventral pathfinding of limb motor axons. Development 127, 3313–3324.

Huber, A.B., 2005. Distinct roles for secreted semaphorin signaling in spinal motor axon guidance. Neuron 48, 949–964.

Huettl, R.E., et al., 2011. Npn-1 contributes to axon-axon interactions that differentially control sensory and motor innervation of the limb. PLoS Biol 9, e1001020.

Iwasato, T., et al., 2007. Rac-GAP alpha-chimerin regulates motor-circuit formation as a key mediator of EphrinB3/EphA4 forward signaling. Cell 130, 742–753.

Jaworski, A., Tessier-Lavigne, M., 2012. Autocrine/juxtaparacrine regulation of axon fasciculation by Slit-Robo signaling. Nat. Neurosci. 15, 367–369.

Kania, A., Jessel, T.M., 2003. Topographic motor projections in the limb imposed by LIM Homeodomain protein regulation of ephrin-A:EphA interactions. Neuron 38, 581–596.

Kao, T.J., Kania, A., 2011. Ephrin-mediated cis-attenuation of Eph receptor signaling is essential for spinal motor axon guidance. Neuron 71, 76–91.

Kao, T.J., et al., 2011. Eph and ephrin signaling: Lessons learned from spinal motor neurons. Semin. Cell Dev. Biol.

Kirkham, D.L., et al., 2006. Neural stem cells from protein tyrosine phosphatase sigma knockout mice generate an altered neuronal phenotype in culture. BMC Neurosci. 7, 50.

Kolodkin, A.L., Tessier-Lavigne, M., 2011. Mechanisms and molecules of neuronal wiring: a primer. Cold Spring Harb. Perspect. Biol. 3, a001727.

Kramer, E.R., et al., 2006. Cooperation between GDNF/Ret and ephrinA/EphA4 signals for motor-axon pathway selection in the limb. Neuron 6, 35–47.

Krull, C.E., et al., 1997. Interactions of Eph-related receptors and ligands confer rostrocaudal pattern to trunk neural crest migration. Curr. Biol. 7, 571–580.

Landmesser, L., Honig, M.G., 1986. Altered sensory projections in the chick hind limb following the early removal of motoneurons. Dev. Biol. 118, 511–531.

Logan, M., et al., 2002. Expression of Cre recombinase in the developing mouse limb bud driven by a Prxl enhancer. Genesis 33, 77–80.

Lowery, L.A., Van Vactor, D., 2009. The trip of the tip: understanding the growth cone machinery. Nat. Rev. Mol. Cell. Biol. 10, 332–343.

Luria, V., et al., 2008. Specification of motor axon trajectory by ephrin-B:EphB signaling: symmetrical control of axonal patterning in the developing limb. Neuron 60, 1039–1053.

Marmigere, F., Ernfors, P., 2007. Specification and connectivity of neuronal subtypes in the sensory lineage. Nat. Rev. Neurosci. 8, 114–127.

Marquardt, T., et al., 2005. Coexpressed EphA receptors and ephrin-A ligands mediate opposing actions on growth cone navigation from distinct membrane domains. Cell 8, 127–139.

Nédelec, S., et al., 2012. Concentration-dependent requirement for local protein synthesis in motor neuron subtype-specific response to axon guidance cues. J. Neurosci. 32, 1496–1506.

Noberini, R., et al., 2012. Profiling Eph receptor expression in cells and tissues: A targeted mass spectrometry approach. Cell Adh. Migr. 6, 102–112. ([Epub ahead of print]).

North, H.A., et al., 2009. Promotion of proliferation in the developing cerebral cortex by EphA4 forward signaling. Development 136, 2467–2476.

Orioli, D., et al., 1996. Sek4 and Nuk receptors cooperate in guidance of commissural axons and in palate formation. EMBO. J. 15, 6035–6049.

Petros, T.J., et al., 2010. Ephrin-B2 elicits differential growth cone collapse and axon retraction in retinal ganglion cells from distinct retinal regions. Dev. Neurobiol. 70, 781–794.

Srivastava, N., et al., 2013. EphB2 receptor forward signaling controls cortical growth cone collapse via Nck and Pak. Mol. Cell Neurosci. 52, 106–116.

Tosney, K.W., Landmesser, L.T., 1985. Development of the major pathways for neurite outgrowth in the chick hindlimb. Dev. Biol. 109, 193–214.

Tsuchida, T., et al., 1994. Topographic organization of embryonic motor neurons defined by expression of LIM homeobox genes. Cell 79, 957–970.

Wang, G., Scott, S.A., 1999. Independent development of sensory and motor innervation patterns in embryonic chick hindlimbs. Dev. Bio. 208, 324–336.

Wang, H.U., Anderson, D.J., 1997. Eph family transmembrane ligands can mediate repulsive guidance of trunk neural crest migration and motor axon outgrowth. Neuron 18, 383–396.

Wang, L., et al., 2011. Anatomical coupling of sensory and motor nerve trajectory via axon tracking. Neuron 71, 263–277.

Wichterle, H., et al., 2002. Directed differentiation of embryonic stem cells into motor neurons. Cell 110, 385–397.